Analysis of Exterior Acoustics using the Edge-based Smoothed Finite Element Method (ES-FEM)

Wei Li [1], Ming Lei [1*], Yingbin Chai [1] and G.R. Liu[2]

1Department of Naval Architecture and Ocean Engineering, Huazhong University of Science and Technology, Wuhan City, P. R. China 430074

2 School of Aerospace Systems, University of Cincinnati, Cincinnati Ohio, 45221

*Corresponding author: hustleiming@163.com

Abstract

Solving acoustic problems governed by Helmholtz equation by standard finite method (FEM), the numerical dispersion error is not negligible when the wave increases due to the "overly-stiff" character of FEM. To overcome this numerical dispersion error, this paper uses the edge-based smoothed finite method (ES_FEM) to analyze the 2D exterior scattering problems. Linear triangle elements and is employed separately to mesh the 2D computational domain. Using gradient smoothing technology to build a relatively soft stiffness thus the numerical dispersion error can significantly decreased. In addition, the gradient smoothing technology transfers domain integrals involving gradient of shape function to simple boundary integrals involving only shape function, which can reduce computing cost. In order to model exterior acoustic problems defined in unbounded domains, the unbounded domain is truncated by an artificial boundary on which the non-reflecting boundary condition is imposed to replace the Somerfield condition at infinite. Examples for exterior scattering problems with known exact solutions are calculated to demonstrate the ES-FEM realization, result shows that the ES-FEM is also very accurate. Compared FEM calculation process and results, ES-FEM is more effective and could achieve much more accurate result in solving exterior acoustic problems, especially when number is large.

Keywords: Smoothed Finite Element Method, Acoustic Scattering, Unbounded Domain, non-reflecting boundary

1. Introduction

Seeking for the numerical solution of acoustic problems governed by Helmholtz equation has been a widely concerned issue in numerical research which aims to improve the computational accuracy and efficiency and applicability of the algorithm. The analytical solution can be derived for simple acoustic problems, but it's difficult to derive analytical solution when acoustic model is relatively complex. Thus it cannot avoid using numerical methods to solve engineering problems. In the past few decades, many numerical methods are extensively used to get approximate solution of acoustic problems (Abboud, 1990; Avorinde, 1990; Dokumacl, 1991; Givoli, 1989 and Gerdes, 2000), especially the standard finite element method (FEM) (Lonny, 2006 and Harari, 2004) and boundary element method (BEM) (Burton, 1971; Colton, 1983 and Walsh, 2004). A known issue is that numerical method including FEM usually generate "numerical dispersion" error which cannot be neglected in high frequency range (the wave number k is large) (Suleau, 2000).

In order to eliminate the numerical dispersion error, researchers has proposed a series of methods. In recent years, element-free technique has been widely used and developed. Belytschko et al., 1994 proposed the element-free Galerkin method (EFGM), but this method is also sensitive to dispersion error. Bouillard et al., 1998 improved EFGM and obtained higher accuracy and better convergence. Petersen et al.

used high-order spectral element shape function to analyze acoustic problems, and it showed that this method lead to higher accuracy and stability as well as good computational efficiency (Petersen, 2006). Harari et al., 2004 applied stabilized finite element method to basic Galerkin form for Helmholtz equation and improved its stability. Although FEM has been widely used to solve acoustic problems, FEM solution shows the lower bound property due to the character of overly-stiff, and on the contrary, NS-FEM solution presents the upper bound property duo to its overly-soft character. In order to artificially control the character of the stiffness, α-FEM (Liu, 2008, 2009a) was proposed with a controlling factor (α) whose value varies between 0 and 1.

In recent several years, smoothed finite element method (ES-FEM) was introduced by Liu et al., 2009b which combines FEM with strain smoothing techniques and it showed that ES-FEM can provide better accuracy and stability because ES-FEM settled the "overly stiff" issue that standard FEM may face. At first, ES-FEM was mainly used to solve solid mechanics problems like free and forced vibration (Dai, 2007; Cui, 2010 and Nguyen, 2010). Result showed that ES-FEM obtained more accurate natural frequency than FEM and thus obtained more accurate stress and strain   Later, ES-FEM was applied to solve acoustic problems and still behaves better than FEM. Z.C.He et al., 2010 studied the coupled problems of structural-acoustic by ES-FEM and successfully alleviated the shear locking phenomenon. Z.CHe et al., 2009 also studied pure acoustic problems governed by Helmholtz equation and demonstrated that ES-FEM achieved better result than FEM.

Since analysis of interior acoustic problems has been researched by SFEM, this paper pays attention on exterior acoustic problems and investigates if SFEM still behaves better than FEM. To solve acoustic problems in unbounded domain, an artificial boundary is usually introduced to make the computational domain finite and impose certain condition on it. Keller and Givoili, 1988 derived an exact non-reflecting boundary condition (the Dirichlet-to-Neumann condition) in case that the artificial boundary is a sphere. Berengers, 1994 proposed perfectly matched layer (PLM) method to solve Maxwell equation in unbounded domain. Local absorbing boundary condition (Wilcox, 1956) and infinite elements (Bettess, 1992) can also be applied to treat the artificial boundary. In this paper DtN boundary condition is used to deal with the artificial boundary.

In this paper, exterior acoustic problems are investigated by ES-FEM, and we further study the efficiency and accuracy of ES-FEM. The organization of this paper is as follows: section 2 is a briefly description of the computational model and a detailed introduction of ES-FEM formulation; section 3 is a comparison of ES-FEM to FEM in three aspects: the computing efficiency, the accuracy and the sensitivity to irregular mesh; section 4 is a demonstration of ES-FEM in practical application; section 5 shows the conclusions derived from the numerical results.

2. Basic theory of ES-FEM for acoustic problem

2.1 Governing equation

For ideal homogeneous fluid, the acoustic wave equation can be described as:

$$\nabla^2 p = \frac{1}{c^2}\frac{\partial^2 p}{\partial t^2}$$

(1)

where ∇^2 represents the Laplace operator, c is the speed of acoustic wave and p is the

acoustic pressure. If the acoustic wave is further time-harmonic, Eq. (1) can be simplified as:

$$\nabla^2 p + k^2 p = 0 \tag{2}$$

where k represents the wave number.

Consider the situation that a scattering object outlined by boundary Γ_1 is located in an infinite domain Ω, solve the scattering field when an incident wave passes by. The problem can be stated as: given boundary condition (such as particle vibration velocity or a description about the velocity) on Γ_1, find acoustic pressure p in domain Ω such that:

$$\nabla^2 p + k^2 p = 0 \qquad \text{in} \ \ \Omega \tag{3}$$

$$\nabla p \cdot n = -j\rho\omega v_n \qquad \text{On} \ \ \Gamma_1 \tag{4}$$

$$\lim_{r \to \infty} r\left(\frac{\partial p}{\partial r} - jkp\right) = 0 \qquad \text{At infinity} \tag{5}$$

where v_n, ω and ρ represent the normal velocity on boundary Γ_1, the angle frequency and the density of the fluid, respectively. Eq. (5) is the Sommerfeld radiation condition which guarantees the positive energy flux at infinity so that the solution is unique. However Eq. (5) is not practicable for numerical method because it requires the mesh to be infinitely vast. An alternative is to introduce an artificial boundary Γ_2 on which impose the following condition:

$$\nabla p \cdot n = -M \cdot p \qquad \text{On} \ \ \Gamma_2 \tag{6}$$

In Eq. (6), M is the Dirichlet to Neumann (DtN) map which describes the relationship between pressure p and its derivative. In 2-D problems when the artificial boundary is a circle, Givoli derived that M could be expressed as:

$$M_n = -\frac{k}{\pi} \frac{\dot{H}_n^{(1)}(kR)}{H_n^{(1)}(kR)} cosn(\theta - \theta') \tag{7}$$

2.2 *Formulation of standard FEM*

To get the weak formulation of Helmholtz equation, firstly multiply test function w to Eq. (1):

$$\int_\Omega w\left(\Delta p + k^2 p\right) d\Omega = 0 \tag{8}$$

Then use Green's theorem to integrate Eq. (8) by parts to obtain:

$$-\int_\Omega \nabla w \cdot \nabla p \, d\Omega + k^2 \int_\Omega w \cdot p \, d\Omega + \int_\Gamma w(\nabla p \cdot n) d\Gamma = 0 \tag{9}$$

Adding the boundary condition Eq. (4) and Eq. (6) to Eq. (9):

$$\int_\Omega \nabla w \cdot \nabla p d\Omega - k^2 \int_\Omega w \cdot p d\Omega + \int_{\Gamma_2} w \cdot M \cdot p d\Gamma_2 = -j\rho\omega \int_{\Gamma_1} w \cdot v_n d\Gamma_1 \qquad (10)$$

Assuming both the acoustic pressure p and the test function w can be expressed approximately as

$$p = \sum_{i=1}^m N_i p_i = NP \qquad (11)$$

where p_i and N_i represent the unknown nodal pressure and FEM shape function, respectively. Applying Eq. (11) to Eq. (10), the discretized system equation is finally obtained as the following matrix form:

$$\{K - k^2 M + K_{AB}^b\} = \{F\} \qquad (12)$$

where K is the FEM stiffness matrix:

$$K = \int_\Omega (\nabla N)^T \cdot \nabla N d\Omega \qquad (13)$$

M is the mass matrix:

$$M = \int_\Omega N^T \cdot N d\Omega \qquad (14)$$

K_{Ab}^b is the boundary matrix:

$$K_{AB}^b = \sum_{n=0}^\infty -\frac{k}{\pi} \frac{\dot{H}_n^{(1)}(kR)}{H_n^{(1)}(kR)} \left(\int_{\Gamma_2} N_A \begin{bmatrix} \cos n\theta & \sin n\theta \end{bmatrix} d\Gamma_2 \right) \left(\int_{\Gamma_2} N_B \begin{bmatrix} \cos n\theta' \\ \sin n\theta' \end{bmatrix} d\Gamma_2 \right) \qquad (15)$$

and F is the force matrix:

$$F = -j\rho\omega \int_{\Gamma_1} N^T v_n d\Gamma_1 \qquad (16)$$

Solving scattering problems, it is common to make the particle vibration velocity of the incident and scattered wave to meet certain conditions on surface of scatters, thus scattering problems is replaced by radiation problems. If the scattering object is rigid, it is granted that particle vibration velocity of the scattered wave V_s is negative to that of the incident wave V_i, namely $V_s = -V_i$. When velocity is complex, $V_s = -conj(V_i)$, which means if the velocity angle phase of the incident wave at point A advances that at point B, so it is the same with the scattered wave.

2.3 Creation of Edge-Based smoothing domain and ES-FEM stiffness matrix

To solve the same acoustic problem, ES-FEM and FEM have exactly the same mass matrix、 boundary matrix and force matrix， the only difference between them lies in the stiffness matrix .ES-FEM introduces the gradient smoothing technique which

replaces the gradient component ∇N with the smoothed item $\overline{\nabla N}$, thus the ES-FEM stiffness matrix can be written as:

$$\overline{K} = \int_{\Omega} \left(\overline{\nabla N}\right)^{T} \overline{\nabla N} d\Omega \tag{17}$$

Assuming the 2-D acoustic domain Ω has been divided into N_e "no-overlap" and "no-gap" triangle elements Ω_i with N_n nodes and N_{eg} edges, such that: $\Omega = \bigcup_{i=1}^{N_e} \Omega_i$ and $\Omega_i \bigcap \Omega_j = 0$, $(i \neq j)$. Find the central point of each element and connect it with its neighbor nodes, therefore the sub-smoothing domain Ω_k^s for edge k is created. Thus the problem domain Ω can further be divided into N_{eg} "no-overlap" and "no-gap" smoothing domains, such that: $\Omega = \bigcup_{k=1}^{N_{eg}} \Omega_k^s$ and $\Omega_i^s \bigcap \Omega_j^s = 0$ $(i \neq j)$. The inner character of smoothing technique for acoustic pressure is smoothing the velocity. For the kth smoothing domain Ω_k^s, the smoothing velocity can be expressed as:

$$\overline{v}(x_k) = \int_{\Omega_k^s} v(x_k) W(x - x_k) d\Omega \tag{18}$$

In which $W(x - x_k)$ is the smoothing function by:

$$W(x - x_k) = \begin{cases} 1/V_k & \left(x \in \Omega_k^s\right) \\ 0 & \left(x \notin \Omega_k^s\right) \end{cases} \tag{19}$$

where $V_k = \int_{\Omega_k^s} d\Omega$ is the area of smoothing domain of edge k. Substituting Eq. (18) into Eq. (17), the domain integration of velocity is transformed into the boundary integration of acoustic pressure:

$$\overline{v}(x_k) = -\frac{1}{j\rho\omega V_k} \int_{\Omega_k^s} \nabla p \, d\Omega = -\frac{1}{j\rho\omega V_k} \int_{\Gamma_k} p \Box n \, d\Gamma \tag{20}$$

The gradient smoothing acoustic pressure can be written as:

$$\overline{\nabla} p = \sum_{I=1}^{N} \overline{B}_I p_I \tag{21}$$

where N is the total number of element surrounding the smoothing edge (for boundary edge $N = 1$, for inner edge $N = 2$) and $\overline{B}_I$ is the gradient smoothing

matrix with $\overline{B}_I = [b_{I1} \quad b_{I2}]$. Substituting shape function into Eq. (20) and using one point Gauss integration method to get

$$b_{Id} = \frac{1}{V_k} \int_{\Gamma_k} N_I n_d d\Gamma = \sum_{i=1}^{N_b} \frac{1}{V_k} N_I \left(x_i^{GP}\right) n_{id} l_i \qquad d = 1, 2 \qquad (22)$$

In which, Γ_k is the boundary of smoothing domain Ω_k^s, N_I the shape function,

N_b the segment number of boundary Γ_k, x_i^{GP} the midpoint of boundary segment,

n_{id} the unit outward vector, l_i the length of boundary segment.

Finally Eq. (17) can be written as:

$$\overline{K} = \sum_{k=1}^{N_{eg}} \int_{\Omega_k} \overline{B}_I^T \overline{B}_I d\Omega \qquad (23)$$

From above it can be found that: for FEM stiffness each node interacts only with the node belonging to the same element, which means the stiffness of each element is only distributed to the nodes belonging to it. In terms of ES-FEM stiffness, each node interacts not only with the node belonging to the same element, but also with the node belonging to its neighbor elements, which indicates that the stiffness of each element is distributed not only to the nodes belonging to it, but also to the nodes belonging to its neighbor elements. This special distribution increases the bandwidth of the stiffness matrix and seams to take more computation cost, but on the contrary ES-FEM introduces smoothing function to the domain integration and transfers it into simple boundary integration which greatly reduces the computation time. Besides that distribution is the way how ES-FEM softens the FEM stiffness and reduce numerical dispersion error caused by overly-rigid stiffness.

3. Numerical solution for 2D problems

In this section, an example with known exact solution is studied to analyze the computing efficiency，accuracy and mesh sensitivity of ES-FEM. Assume a rigid cylinder of infinite length is located in an unbounded domain, use both ES-FEM and FEM to solve the scattering pressure field when a plane wave passes by. The computation domain is the area surrounded by two circular boundary, one is the outline of the cylinder with radius a=0.2m and the other is the artificial boundary with radius R=1m. Assume the plane wave is propagating along the x-axis with the following formulation:

$$P_i = \exp\left(-jkx\right) \qquad (23)$$

The exact solution of this scattering problem can be expressed by the following formulation:

$$P_s = \sum_{n=0}^{\infty} \left[-(-j)^n \varepsilon_n \frac{\dfrac{d}{d(ka)} J_n(ka)}{\dfrac{d}{d(ka)} H_n^{(2)}(ka)} \right] H_n^{(2)}(kr) \cos(n\theta) \qquad (24)$$

In Eq. (24), when n=0, $\varepsilon_n = 1$ otherwise $\varepsilon_n = 2$, $J_n(x)$ and $H_n(x)$ are Bessel function of the first and third (Hankel function) kind.

3.1 Computing efficiency comparison

The main and the only difference of ES-FEM and FEM in solving the same problem is the global stiffness matrix. Therefor to evaluate the computing efficiency of ES-FEM and FEM is to compare their computing time on calculating the global stiffness matrix. It is common sense that differentiation and integration operator is much more time-costing than basic arithmetic operator such as addition and multiplication. Comparing to FEM, ES-FEM prevails in that ES-FEM does not need to perform differentiation even though the formulation has an item of ∇N, because the smoothing technology is introduced to transform the domain integration of ∇N into boundary integration of N as shown in Eq. (19). Thus the integration of ES-FEM is one-dimensional while the integration of FEM is two-dimensional which also reveals the advantage of ES-FEM in computing cost.

Use ANSYS mesh generator to mesh the computation domain, and set the mesh size to get five different models with 576,1196,1620,2176 and 2660 nodes, each model being meshed by both T3 and Q4 element. The global stiffness matrix of both ES-FEM and FEM are programmed and computed by MATLAB whose version is MATLAB 2010 and the computing time result are listed in Table 1. Note that the main hardware equipment of the computer is as follows: Intel(R) Xeon(R) CPU E3-1230 V2 @ 3.30GHz, Intel(R) 7series /C 216 Chipset Family USB Enhanced Host Controller and ACPI x64-based PC.

It can be obviously observed from Table 1 that: (1) regardless of the element type, computing of both ES-FEM and FEM are linearly increasing with the total number of nodes; (2) for model of the same nodes, computing speed of ES-FEM is approximately 40 times faster than that of FEM in terms of T3 element, and1400 times faster in terms of Q4 element; (3) the computing time of ES-FEM is less effected by element type than that of FEM. The detailed reason why ES-FEM computes faster than FEM lies in that: (1) ES-FEM does not need to perform differentiation or integration for both T3 and Q4 element; (2) for T3 element, FEM does not need to perform integration because ∇N is constant; (3) for Q4 element, FEM needs to perform both differentiation and integration, and the integration is numerically solved by Gaussian integral with two Gauss points in each dimension. It can be concluded from above that ES-FEM behaves much better than FEM does in computing efficiency.

Table 1. Computing time of the global stiffness matrix using ES-FEM and FEM, T3 means triangular element and Q4 means quadrilateral element

Total node number	ES-FEM(T3) (s)	FEM(T3) (s)	ES-FEM(Q4) (s)	FEM(Q4) (s)
576	0.17	57.01	0.75	1034.28
1196	0.30	126.14	1.66	2254.13
1620	0.41	180.24	2.33	3325.81
2176	0.57	205.50	3.60	4955.62
2660	0.71	270.33	4.48	5250.75

3.2 Accuracy comparison

From last section it concludes that ES-FEM is more efficiency than FEM, this section focuses on the accuracy of ES-FEM. The accuracy of ES-FEM is investigated and the result comparison with FEM is mainly conducted in the following three aspects:

Firstly, for certain wave number, compare the numerical result of ES-FEM and FEM with the exact solution. To demonstrate scattering properties, pressures of nodes on artificial boundary are picked to be plotted in Fig.1, where (a), (b) and (c) are corresponding to low frequency ($ka=\pi$), medium frequency ($ka=2\pi$) and high frequency ($ka=3\pi$). It is shown that both ES-FEM and FEM could achieve acceptable result on the whole and ES-FEM result is as same accurate as FEM result in terms of backward scattering. Besides, ES-FEM obtains more accurate result than FEM in terms of forward scattering, especially at petal-like corner. In order to demonstrate the accuracy of ES-FEM, special attention will be paid on forward scattering.

（a）$ka=\pi$ （b）$ka=2\pi$

（c）$ka=3\pi$
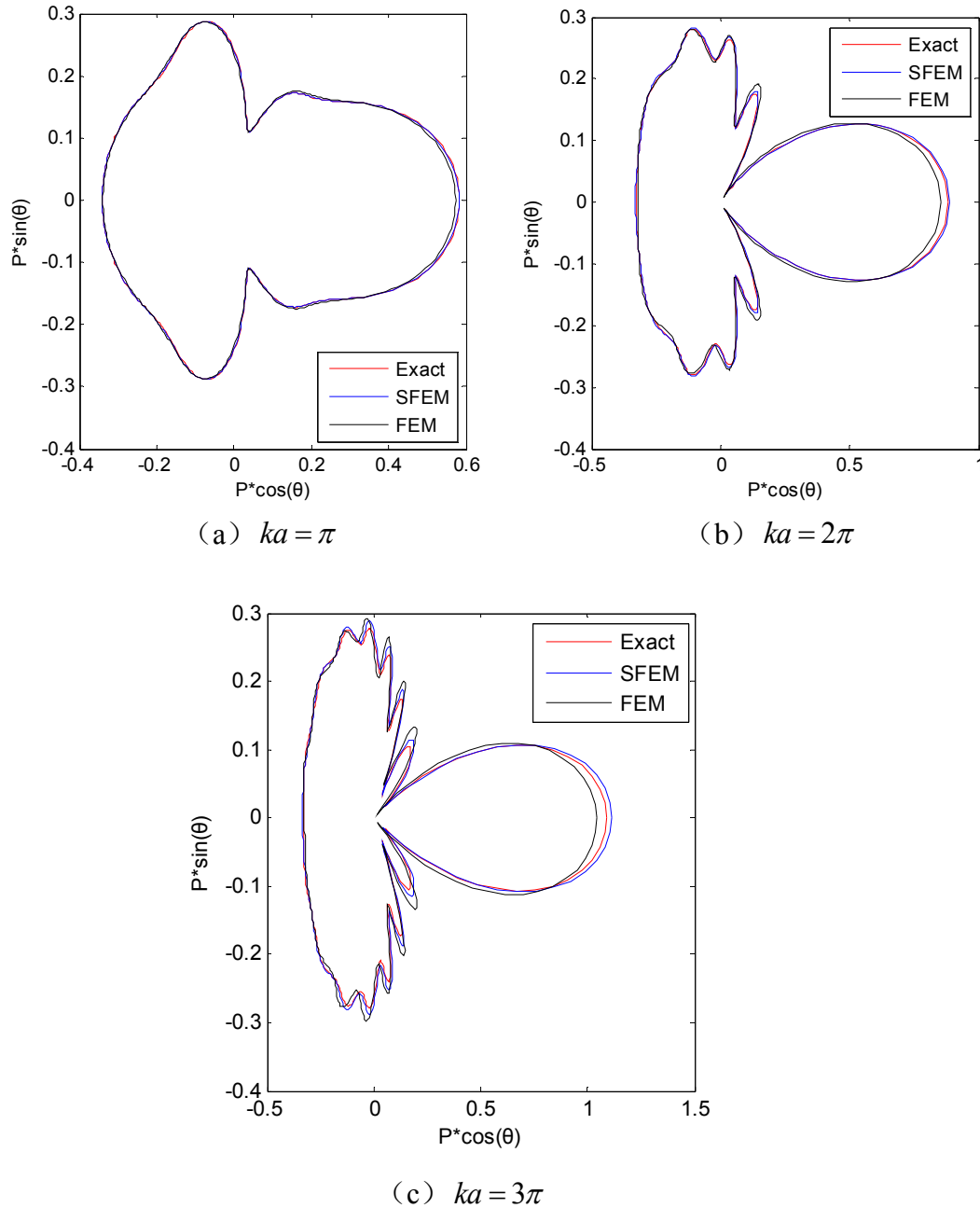
Figure 1. Pressure distribution on artificial boundary at different wave number

Secondly, for certain scattering angle, how the scattering pressure varies with non-dimensional number is investigated and behavior of ES-FEM and FEM is observed. Nodes on artificial boundary at angle of $0°$, $30°$, $60°$ and $90°$ are picked to demonstrate the comparison which are plotted in Fig.2. It is shown that: (1)

at low frequency band, numerical results of both ES-FEM and FEM are exactly the same as the exact solution; (2) at high frequency band, ES-FEM result is more close to exact solution than FEM result although error of both ES-FEM and FEM becomes larger as frequency increases.

Finally, separately observe the real part and the image part of the pressure result since the scattering field is complex. Pressures of nodes on artificial boundary at several scattering angles are picked for the comparison and the results are listed in Table 2, Table 3 and Table 4.

（a）Scattering angle 0°   （b）scattering angle 30°

（c）scattering angle 60°   （d）scattering angle 90°
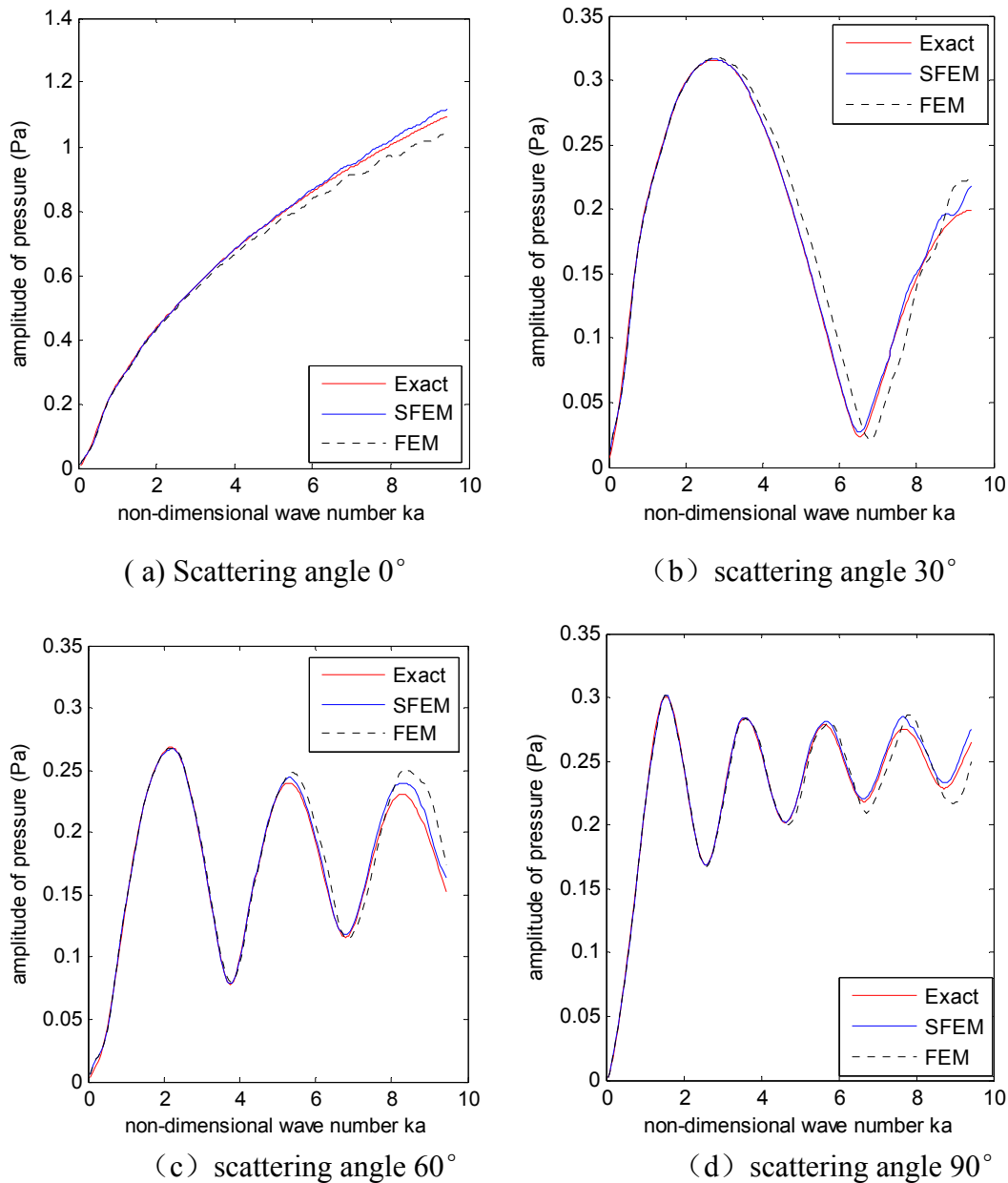
Figure 2. Pressure variation with wave number at certain scattering angle

It can be observed that both the real part and the image part of ES-FEM result pressure are very close to that of the exact solution in case of low frequency, medium frequency and even high frequency. In terms of FEM result, the amplitude of pressure is close to the exact solution, but neither the real part nor the image part of the pressure is very close to the exact solution. It can be concluded that: (1) for ES-FEM, the real part, the image part and the amplitude of the result pressure are all very

approximate to the exact solution; (2) for FEM, only the amplitude of the pressure is approximate to the exact solution while the real part and the image part of the pressure is less accurate than ES-FEM at low frequency and not stable at high frequency; (3) ES-FEM has better convergence and accuracy than FEM.

Table 2. Pressures of nodes on artificial boundary at different scattering angle when non-dimensional wave number $ka = \pi$.

Scattering angle	Exact (Pa)	ES-FEM result (Pa)	FEM result (Pa)
0.00°	0.3265 + 0.4839i	0.3262 + 0.4861i	0.3036 + 0.4901i
10.25°	0.3222 + 0.4289i	0.3220 + 0.4306i	0.3023 + 0.4360i
20.51°	0.3093 + 0.2875i	0.3094 + 0.2881i	0.2974 + 0.2970i
30.75°	0.2505 - 0.0197i	0.2512 - 0.0214i	0.2562 - 0.0073i
39.87°	0.2589 + 0.0008i	0.2597 - 0.0008i	0.2636 + 0.0133i
50.13°	0.2162 - 0.0566i	0.2170 - 0.0585i	0.2236 - 0.0454i
60.38°	0.1616 - 0.0268i	0.1622 - 0.0282i	0.1664 - 0.0193i
70.63°	0.0971 + 0.0630i	0.0973 + 0.0625i	0.0963 + 0.0655i
79.75°	0.0350 + 0.1565i	0.0349 + 0.1568i	0.0287 + 0.1551i
90.00°	-0.0352 + 0.2384i	-0.0356 + 0.2392i	-0.0459 + 0.2340i

Table 3. Pressures of nodes on artificial boundary at different scattering angle when non-dimensional wave number $ka = 2\pi$.

Scattering angle	Exact (Pa)	ES-FEM (Pa)	FEM (Pa)
0.00°	-0.6371 - 0.6103i	-0.6361 - 0.6247i	-0.4119 - 0.7495i
10.25°	-0.5159 - 0.4272i	-0.5151 - 0.4350i	-0.3708 - 0.5489i
20.51°	-0.2512 - 0.0955i	-0.2504 - 0.0925i	-0.2442 - 0.1727i
30.75°	0.1055 - 0.1056i	0.1081 - 0.1078i	0.1413 - 0.0632i
39.87°	0.0895 - 0.0718i	0.0918 - 0.0723i	0.1061 - 0.0380i
50.13°	0.1388 - 0.1727i	0.1419 - 0.1788i	0.2142 - 0.1125i
60.38°	0.1427 - 0.0627i	0.1448 - 0.0665i	0.1735 - 0.0152i
70.63°	0.0854 + 0.1619i	0.0854 + 0.1646i	0.0259 + 0.1732i
79.75°	-0.0255 + 0.2620i	-0.0272 + 0.2676i	-0.1186 + 0.2405i
90.00°	-0.1693 + 0.1676i	-0.1718 + 0.1703i	-0.2166 + 0.1170i

Table 4. Pressures of nodes on artificial boundary at different scattering angle when non-dimensional wave number $ka = 3\pi$.

Scattering angle	Exact (Pa)	ES-FEM (Pa)	FEM (Pa)
0.00°	0.8957 + 0.6257i	0.8940 + 0.6713i -	0.0210 + 1.0468i
10.25°	0.4843 + 0.3266i	0.4766 + 0.3394i	0.0655 + 0.6087i
20.51°	-0.0811 + 0.0316i	-0.0972 + 0.0187i	0.0161 + 0.0076i
30.75°	-0.0506 + 0.0036i	-0.0518 + 0.0077i	-0.0674 - 0.0604i
39.87°	-0.0654 + 0.0632i	-0.0693 + 0.0723i	-0.1392 - 0.0521i
50.13°	0.0042 - 0.1933i	0.0138 - 0.2064i	0.2010 - 0.0575i
60.38°	0.1262 - 0.0857i	0.1374 - 0.0888i	0.1582 + 0.0755i

70.63°	0.0996 + 0.2164i	0.0997 + 0.2303i	-0.1640 + 0.1747i
79.75°	-0.1198 + 0.1812i	-0.1278 + 0.1877i	-0.2392 + 0.0023i
90.00°	-0.2345 - 0.1232i	-0.2412 - 0.1349i	0.03 - 0.2509i

3.3 Sensibility to irregular mesh

Since the computation domain boundary is curved, no mesh generator can produce 100% equilateral triangle elements. Use element quality statistics to evaluate the irregularity of the whole mesh, and the quality of each element is evaluated by the following expression:

$$Q = \frac{3\alpha_{min}}{\pi} \tag{25}$$

where α_{min} is the minimum inner angle of the triangle and Q is a number between 0 and 1, 1 stands for equilateral triangle and 0 the worst element.

The original mesh data is automatically obtained by ANSYS mesh generator and the irregular mesh data is generated programmatically by the following expression:

$$x' = x + \Delta x \cdot r_c \cdot \beta_{ir} \tag{26}$$

$$y' = y + \Delta y \cdot r_c \cdot \beta_{ir} \tag{27}$$

where r_c is a random number between -1.0 and 1.0 and β_{ir} is the irregularity degree whose value varies between 0 and 0.5. The larger value of β_{ir} brings about more irregular element distribution. Table 1 shows the element quality statistics of both original mesh data and the irregular mesh data varying with β_{ir}. Element quality statistics of original mesh and irregular mesh is listed in Table 5 from and it can be found that the percentage of worst element increases with irregularity degree while the percentage of best element decreases as expected.

Table 5. Element quality statistics with different irregularity degree β_{ir}

Q	Percentage of worst element ←------------------------------------→ percentage of best element								
	0~0.1	0.1~0.2	0.2~0.3	0.3~0.4	0.4~0.5	0.5~0.6	0.6~0.7	0.7~0.8	0.8~0.9	0.9~1.0
Orignal mesh	—	—	—	—	—	0.01%	6.88%	20.36%	35.38%	37.37%
β_{ir}=0.1	—	—	—	—	—	0.43%	10.77%	23.38%	34.78%	30.64%
β_{ir}=0.2	—	—	—	0.01%	0.51%	4.82%	15.31%	27.97%	33.02%	18.35%
β_{ir}=0.3	—	—	0.01%	0.54%	3.64%	10.72%	20.17%	27.11%	26.54%	11.28%

β_{ir}=0.4	0.02%	0.10%	0.69%	2.94%	7.95%	15.34%	21.09%	24.20%	19.90%	7.77%
β_{ir}=0.5	0.19%	0.79%	2.88%	6.64%	10.79%	16.40%	20.31%	19.80%	16.28%	5.92%
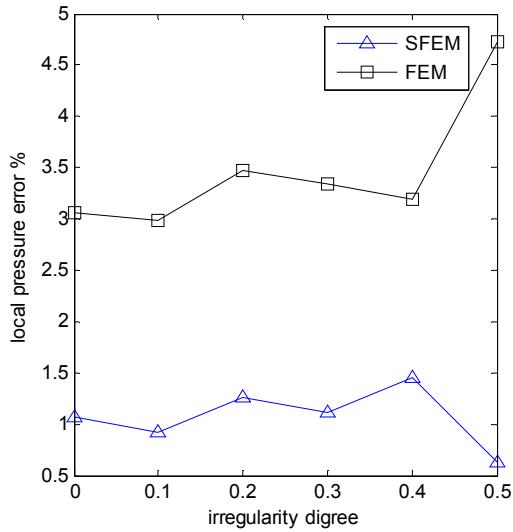
(a) Scattering angle is 0°
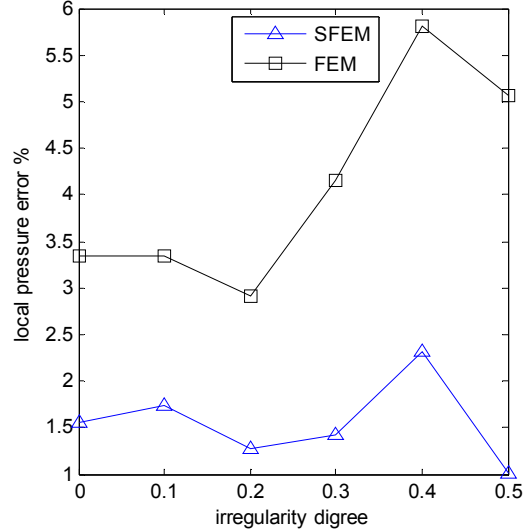
(b) scattering angle is 90°
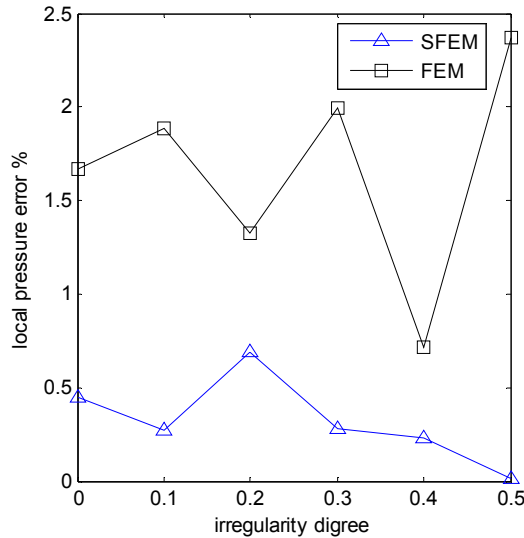
(c) Scattering angle is 180°

Figure 3. Local pressure error varies with the irregularity degree of mesh at certain scattering angle

In order to investigate the sensibility of ES-FEM, five models with irregularity varies between 0.1 and 0.5 are generated for computation and for each model both ES-FEM solution and FEM solution are computed for purpose of comparison. The study is performed at medium frequency when non-dimensional wave $ka = 2\pi$, and local pressure error of node on artificial boundary at scattering angle of 0°, 90° and 180° are calculated which are plotted in Fig.3. The pictures shows that: (1) ES-FEM has lower local pressure error than FEM on the whole; (2) local pressure error of

ES-FEM changes only a little as irregularity degree increases, and achieves even less error when irregularity is 0.5 compared with result from original mesh;(3) local pressure error of FEM has more visible change than ES-FEM as irregularity degree increases, and in general local pressure error becomes larger as irregularity degree increases.

4. Exterior acoustic problem for 2D rudder

Form above it can be found that ES-FEM has more efficiency and accuracy than FEM in solving scattering problem by a circular object. In this section, pressure distribution of a scattering field is studied by ES-FEM and FEM solution. The scattering field is formed by the outline of a 2D rudder and a circular artificial boundary with radius R=3m. It is difficult to derivate the exact solution for this problem since the curve of the 2D rudder is complicated, and the FEM solution of a very fine mesh is taken as the reference solution. For sake of simplicity, assume the density of the fluid media is 1000 kg/m^3 and the wave velocity is 1500 m/s. The computation domain is meshed by linear triangular element with average mesh size h of 0.05 and 0.2m. The former mesh size generates 12970 nodes and 25451 elements, being used to compute reference solution. The latter mesh size generates 1575 nodes and 3007elements, being used to compute ES-FEM solution and FEM solution for comparison.

The acoustic pressure distribution of the problem domain is plotted in Figure 4 when wave number $k = \pi$, where (a), (b) and (c) are respectively obtained by FEM (12970 nodes), ES-FEM (1575 nodes) and FEM (1575 nodes). Similarly, the acoustic pressure distribution in case of wave number $k = 2\pi$ and $k = 3\pi$ are plotted in Figure 5 and Figure 6. From figure 4 it is found that both ES-FEM and FEM solution are very approximate to the reference solution when wave number satisfying "the rule of thumb", which requires $kh < 1$ guaranteeing the accuracy. From Figure 5 it is found that ES-FEM solution is obviously more close to the reference solution than FEM solution when wave number is approaching the limit value according to "the rule of thumb". Figure 6 shows that ES-FEM solution is still acceptable comparing to reference solution even though the wave number breaks "the rule of thumb", while FEM solution departs a lot from the reference solution. This numerical example illustrates that ES-FEM could achieve more accurate result than FEM using the same mesh and calculate higher frequency.

（a）Reference solution
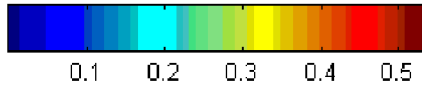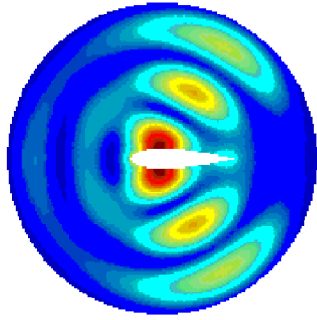
(a) Reference solution
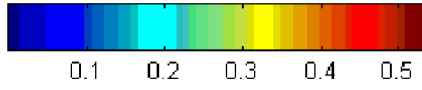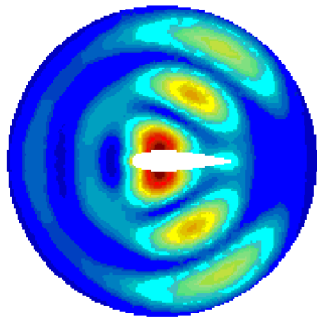

（b）ES-FEM solution
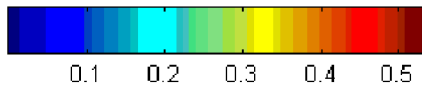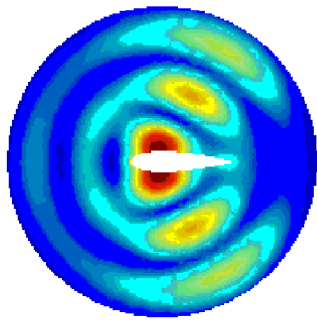
(b) ES-FEM solution

(c) FEM solution

**Figure 4. Pressure distribution when wave number** $k = \pi$
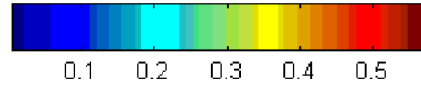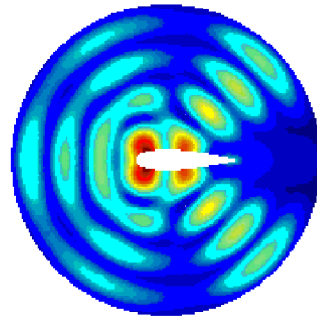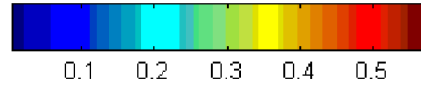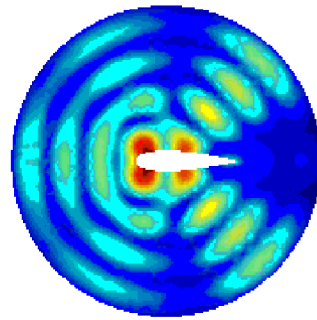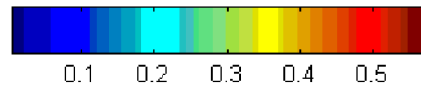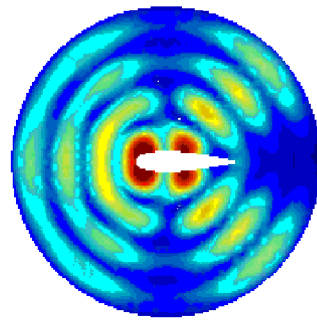
(c) FEM solution

Figure 5. Pressure distribution when wave number $k = 1.5\pi$
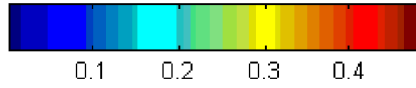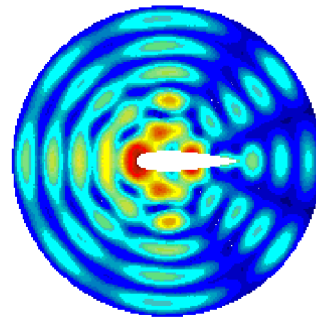
(a) Reference solution
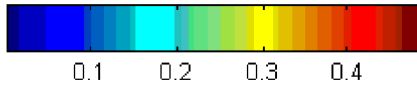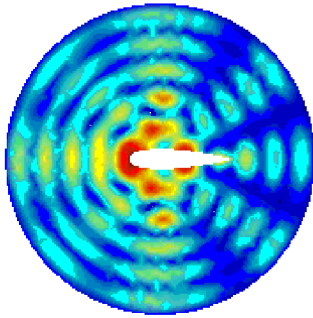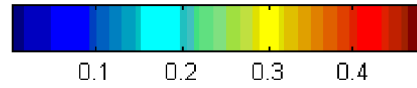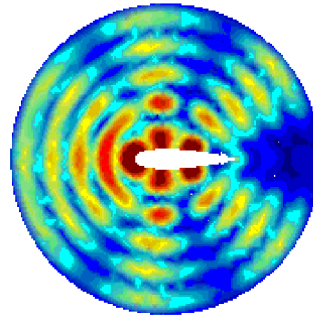
(b) ES-FEM solution　　　　　　(c) FEM solution

Figure 6. Pressure distribution when wave number $k = 2\pi$**.**

5. Conclusions and discussions

In this paper, T3 element is used to investigate 2D exterior scattering problem. MATLAB program code for FEM and ES-FEM is written to calculate the scattering field generated by an infinitely-long cylinder and a 2D rudder. The computation efficiency, accuracy and sensibility to irregular mesh of ES-FEM are studied and its comparison to FEM is also made. Conclusions could be derived as follows:

(a) Solving 2D exterior acoustic problems, ES-FEM is more efficient than FEM in that ES-FEM creates no extra degrees of freedoms and transfers differentiation and integration into simple arithmetic operator when computing global stiffness matrix.

(b) Comparing to analytical solution, both the global and local pressure results of ES-FEM is more accurate than that of FEM. Especially in high wave number, FEM result departs a lot from analytical solution while ES-FEM result is still accurate.

(c) ES-FEM is less sensitive to the mesh irregularity than FEM.

(d) For practical scattering problems, ES-FEM result is more accurate FEM result with the same mesh which suggests that ES-FEM is of great practical value for the future.

References

Abboud, N.N. and P.M. Pinsky (1990), Finite element solution and dispersion analysis for transient structural acoustics problem. *Appl. Mech. Rev*. 43 (5), pp. 381-388.

Avorinde, E.O. (1990), Cylinder structural acoustic vibration by finite element method. *Struct. Compos: Design. Process*. *Technol*, pp. 507-514.

Dokumacl, E. (1991), An integral equation formulation for boundary element analysis of acoustic radiation problems in viscous fluids. *J. Sound Vib.* 147 (2), pp. 335-348.

Givoli, J.B.Keller (1989), A finite element method for large domains. *Comput Meth Appl Mech Engrg*.

Gerdes, K. (2000), A review of infinite element methods for exterior Helmholtz problems. *J. Comput. Acoust*.

Lonny, L. Thompson (2006), A review of finite-element methods for time-harmonic acoustics. *Acoustical Society of America*, pp. 1315-1330.

Harari, I., Magoules, F. (2004), Numerical investigations of stabilized finite element computations for acoustics. *Wave Motion*, pp. 339-349.

Burton, A. and Miller, G. (1971), The application of integral equation methods to the numerical solution of some exterior boundary-value problems. *Proc. R. Soc. London, Ser*. 323, pp. 201-210.

Colton, D. and Kreiss, R. (1983), Integral equation methods in scattering theory. *Wiley-Interscience, New York*.

Walsh, T., Demkowicz and Charles, R. (2004), Boundary element modeling of external human auditory system. *J. Acoust Soc Am*, 115(3), pp. 1033-1043.

Suleau, S., Deraemaeker, A. (2000), Dispersion and pollution of meshless solution for the Helmholtz equation. *Comput Meth Appl Mech Engrg*, 190, pp. 639-657.

Petersen, S., Dreyer, D. and Estorff, O.V. (2006), Assessment of finite and spectral element shape function or efficient iterative simulation of interior acoustics. *Comput. Meth. Appl. Mech Engrg*, 195, pp. 6463-6478.

Harari, I., Magoules, F. (2004), Numerical investigations of stabilized finite element computations for acoustics. *Wave Motion*, 39, pp. 339-349.

Belytschko, T., Lu, Y.Y. and Gu, L. (1994), Element-free Galerkin methods, *Nune Meth Engrg*, 37, pp. 229-256.

Bouillard, Ph. and Suleau, S. (1998), Element-free Galerkin solutions for Helmholtz problems: formulation and numerical assessment of the pollution effect. *Comput Meth Appl Mech Engrg*, 162, pp. 317-335.

Liu, G.R., Nguyen T.T. and Lam K.Y. (2008), A novel alpha finite element method (αFEM) for exact solution to mechanics problems using triangular and tetrahedral elements. *Comput Meth Appl Mech Engrg*, pp. 3883-3896.

Liu, G. R., Nguyen-Xuan, H. and Nguyen-Thoi, T. (2009a), A novel Galerkin-like weak form and a super convergent alpha finite element method (S alpha FEM) for mechanics problems using triangular meshes. *Journal of Computational Physics*, 228, pp. 4055-4087.

Liu, G.R., Nguyen T.T. and Lam, K. Y. (2009b), An edge-based smoothed finite element method (ES-FEM) for static free, and forced vibration analysis. J. *Sound Vib*, 320, pp. 1100-1130.

Cui, X.Y., Liu, G.R., Li, G.Y. and Zhao, X. (2010), Analysis of plates and shells using edge-based smoothed finite element method. *Comput Mech*, 45, pp. 141-156.

Dai, K.Y., Liu, G.R. (2007), Free and forced vibration analysis using the smoothed finite element method (SFEM). J. *Sound Vib*, 301, pp. 803-820.

Nguyen-Xuan, H., Liu, G.R., Thai-hoang, C. and Nguyen-Thoi, T. (2010), An edge-based smoothed finite element mothod (ES-FEM) with stabilized discrete shear gap technique for analysis of Reissner-Mindlin plates, *Comput Meth Appl Mech Engrg*, 199, pp. 471-489.

He, Z.C., Liu, G.R., Zhong, Z.H., Zhang, G.Y., Cheng, A.G. (2010), Coupled analysis of 3D structural-acoustic problems using the edge-based smoothed finite element method/finite element mehod. Finite Elements in Analysis and Design, 46, pp. 1114-1121.

He, Z.C., Liu, G.R., Zhong, Z.H., Wu, S.C., Zhang, G.Y. and Cheng, A.G. (2009), An edge-based smoothed finite element method (ES-FEM) for analyzing three-dimensional acoustic problems. *Comput Meth Appl Mech Engrg*, 199, pp. 20-23.

Keller, B. and Givoli, D. (1988), Exact non-reflecting boundary conditions. *J. Comput. Phys*, 82, pp. 172-192.

Berenger, J.P. (1994), A perfectly matched layer for the absorption of electromagnetic waves. *J. Comput. Phys*, 114(2), pp. 195-200.

Wilcox, C.H. (1956), An expansion theorem for electromagnetic fields. Commun. Pure Appl. Math, 9, pp. 115-134.

Bettess, P. (1992), Infinite elements, Int. J. Numer. Methods Eng, 11(1), pp. 53-64.